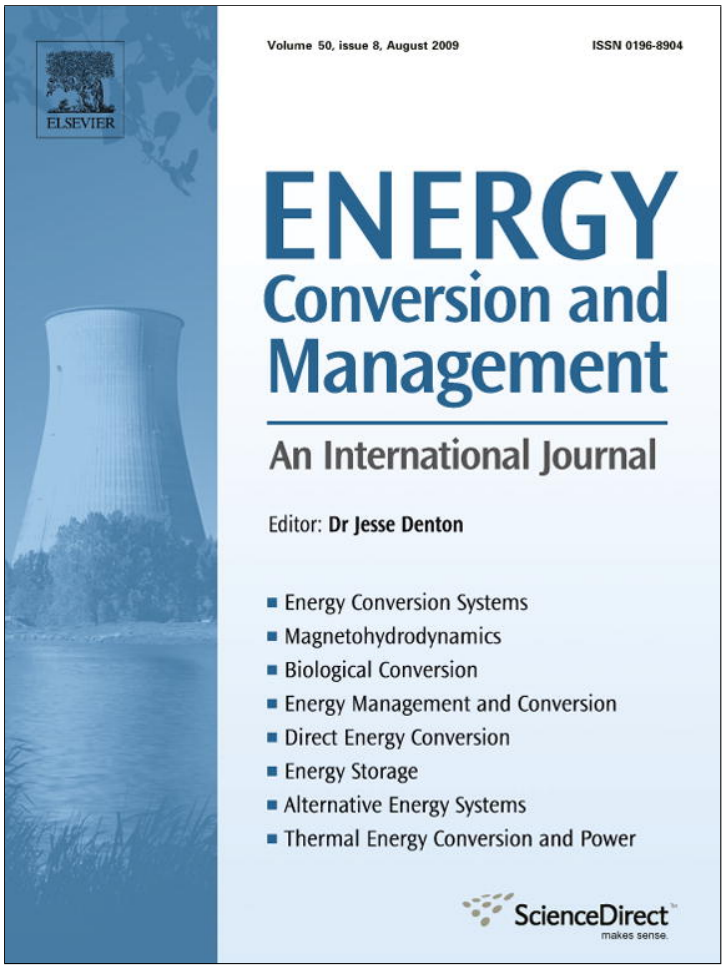

Energy Conversion and Management 50 (2009) 1871–1878

Contents lists available at ScienceDirect

Energy Conversion and Management

journal homepage: www.elsevier.com/locate/enconman

Reliable one-dimensional approximate solutions for insulated oblate spheroid containers

Tsung-Lieh Hsien [a], King-Leung Wong [b,*], Wen-Li Chen [b], Chao-chuan Siao [b]

[a] Department of Electrical Engineering, Kun-Shan University of Technology, 949, Da-Wan Road, Yung-Kang City, Tainan County 710, Taiwan, ROC
[b] Department of Mechanical Engineering, Kun-Shan University of Technology, 949, Da-Wan Road, Yung-Kang City, Tainan County 710, Taiwan, ROC

ARTICLE INFO

Article history:
Received 20 September 2008
Accepted 27 April 2009
Available online 22 May 2009

Keywords:
Insulation
Oblate spheroid
RPSWT model
Integral method

ABSTRACT

Since there is no reliable surface-area formula available for the calculation of the heat-transfer characteristics of an insulated oblate spheroid, in this investigation, highly accurate oblate spheroid surface area is obtained by a simple numerical integration method. Based on the accurate oblate spheroid surface area, a reliable one-dimensional approximate solution of an insulated oblate spheroid container can be obtained with a one-dimensional *RPSWT* model. By comparing with accurate three-dimensional numerical results, it is found that in cases of low external convective coefficient (h_o = 8.3 W m^{-2} K^{-1}), long–short-axes ratio $a/b \leqq 3$, and insulation thickness $t/R_2 \leqq 2$, errors are within 3%. In rarer situations with $a/b \leqq 5$ and $t/R_2 \leqq 2$, the errors are within 5.5%. The above results are almost independent with the internal flow convective coefficient (h_i from 30 to 10^5 W m^{-2} K^{-1}) and dimensionless container size ($0.5R_2h_o/Ks$ from 1.55 to 155).

1. Introduction

The insulation of hot and cold ducts and containers has been one of the most important engineering problems. Yet, simple constant surface area plate thermal resistance (*PTR*) model [1–5] has long been the main stream method to analyze the heat-transfer characteristics of insulated polygonal ducts or polyhedron containers. This model assumes that the insulated surface area of the external insulation is the same as that of a bare duct or container, a practice neglecting the excessive surface area caused by insulation layer thickness, which in turn significantly reduces the magnitude of heat transfer rate. Chou and Wong [6] proposed a plane wedge thermal resistance (*PWTR*) model aimed to investigate the heat-transfer characteristics associated with insulated polygonal pipes. Wong et al. [7] proved that the *PWTR* model can be applied to complete heat-transfer characteristics of insulated polygonal pipes associated with any boundary conditions. In general, if the one-dimensional *PWTR* model [6,7] is used to analyze the two-dimensional heat-transfer problems of insulated polygonal ducts, accuracy deteriorates with decreasing the number of edges. Therefore, Wong et al. [8] studied the heat-transfer characteristics of an insulated long rectangular or square duct using the one-dimensional *PWTR* model and *PTR* model as well as a numerical method. They found that the errors generated by the *PWTR* model are all positive and those generated by the *PTR* model are all negative. Then a 64-*CPWTR* model (combined 60% *PWTR* and 40% *PTR* models) can balance the positive and negative errors and return reasonably accurate results in comparison with two-dimensional numerical solutions. Wong et al. [9] used the same concept to propose a reliable simple one-dimensional 46-*CPWTR* model applied to the two-dimensional heat transfer problem of an insulated triangular duct. Later, Wong et al. [10] extended the various *CPWTR* models to obtain a reliable one-dimensional model for insulated regular polygonal ducts.

As far as an insulated container is concerned, Wong et al. [11] used the optimum interior area thermal-resistance model to analyze the heat-transfer characteristics of an insulated container with arbitrary shape. Wong and Chou [12] also developed a solid wedge thermal resistance (SWTR) model to calculate the heat-transfer characteristics of an insulated cube. Wong et al. [13] proved that the SWTR model can be applied to an insulated cube tank with a wide variety of boundary conditions. Later, Wong and Chou [14] developed a regular polygonal-top solid wedge thermal-resistance (*RPSWT*) model to obtain the heat-transfer characteristics of an insulated regular polyhedron; and Lee et al. [15] proved that the *RPSWT* model can be applied to obtain complete heat-transfer characteristics of an insulated regular polyhedron with extensive boundary conditions. Chen et al. [16] used combined 60% *RPSWT* model and 40% *PTR* model to obtain a reliable one-dimensional method applied to heat-transfer problems associated with insulated rectangular tanks. Chen and Wong [17] also developed a reliable analytical method applied to heat-transfer problems associated with insulated cylindrical tanks.

Recently, Chen et al. [18] proposed a reliable model for an insulted oval duct using one-dimensional *PWTR* model and 91-*CPWTR* model based on very accurate oval perimeter obtained by

* Corresponding author. Tel.: +886 62057121; fax: +886 62050509.
E-mail address: klwong@mail.ksu.edu.tw (K.-L. Wong).

0196-8904/$ - see front matter © 2009 Elsevier Ltd. All rights reserved.
doi:10.1016/j.enconman.2009.04.032

Nomenclature

A	half-long-axis length of cross section profile of oblate spheroid
b	half-short-axis length of cross section profile of oblate spheroid
A_{E1}	internal surface area of an oblate spheroid calculated by accurate numerical integration method
A_{E2}	external surface area of an oblate spheroid calculated by accurate numerical integration method
A_{E3}	external surface area of an insulated oblate spheroid calculated by accurate numerical integration method
A_{C1}	inside surface area of a equivalent sphere based on accurate external surface area of a bare oblate spheroid
A_{C2}	external surface area of a equivalent sphere based on accurate external surface area of a bare oblate spheroid
A_{C3}	external surface area of an insulted equivalent sphere based on accurate external surface area of a bare oblate spheroid
E_C	heat transfer rate error of an insulted equivalent sphere based on accurate external surface area of a bare oblate spheroid
E_W	heat transfer rate error of an insulated oblate spheroid based on accurate area surface and with *RPSWT* model
E_L	error of approximate oval perimeter compared with accurate oval perimeter
E_S	error of approximate oblate spheroid surface area generated by an unsuitable formula
h_i	internal heat convection coefficient
h_o	external heat convection coefficient
K_1	conductivity of wall
K_s	conductivity of insulation layer
$2K_s/h_o$	critical radius of insulated sphere
n	the divided section numbers of oval cross section profile
N	the normal direction of adiabatic boundary
Q_C	heat transfer rate of an insulted equivalent sphere based on accurate external surface area of a bare oblate spheroid
Q_W	heat transfer rate of an insulated oblate spheroid based on accurate area surface and with *RPSWT* model
R_2	outer radius of equivalent sphere based on accurate external surface area of a bare oblate spheroid
$0.5R_2h_o/K_s$	dimensionless container size
RPSWT	regular polygonal-top solid wedge thermal-resistance
S	approximate oval perimeter
t	thickness of insulation layer
t_1	thickness of oblate spheroid container
T_i	temperature of the fluid inside the oblate spheroid container
T_o	temperature of the fluid outside the oblate spheroid container
X	x-coordinate of a rectangular coordinates
Y	y-coordinate of a rectangular coordinates
Z	z-coordinate of a rectangular coordinates

a simple numerical integration method. In the present investigation, a follow-up study to Chen et al. [18], the results are calculated by one-dimensional *RPSWT* model [14,15] based on highly accurate oblate spheroid surface areas calculated by a reliable simple numerical integration method extended from Chen et al. [18]. The results are compared with those of three-dimensional numerical results for insulated oblate spheroid containers with different long–short-axes ratios, from 1.5 to 5, and with three group dimensionless container sizes and in several practical thermal conditions.

2. Problem formulation

Fig. 1 shows the bare oval cross-sectional profile at x–y coordinates of an insulated oblate spheroid container with the external half-long-axis length of a, half-short-axis length of b, wall thickness of t_1, wall conductivity of K_1. An insulation layer with thickness of t and conductivity of K_s is wrapped around the oblate spheroid. The oblate spheroid is then assumed to be exposed to internal and external fluids with convection heat transfer coefficients of h_i and h_o and temperatures of T_i and T_o, respectively. In addition, Fig. 2 shows that various oblate spheroid containers with different long–short-axes ratios a/b of 1.5, 2, 3, 4 and 5, transformed from a bare sphere with the same external surface area, are analyzed in this study.

2.1. The oblate spheroid container's surface area

The following approximate oval perimeter formula [19] has been conventionally used to analyze the characteristics of oval duct:

$$L = 2\pi\sqrt{\frac{a^2+b^2}{2}} \tag{1}$$

The equation of the oval cross-sectional profile of an oblate spheroid container shown in Fig. 3 is

$$\frac{x^2}{a^2}+\frac{y^2}{b^2}=1 \tag{2}$$

The perimeter of the oval cross-sectional profile can then be divided into n line segments. As shown in Fig. 3, the two end points for the ith line segment can be expressed as

$$x_i = a\cos(2i\pi/n) \tag{3}$$

$$y_i = b\sin(2i\pi/n) \tag{4}$$

$$x_{i+1} = a\cos[2(i+1)\pi/n] \tag{5}$$

$$y_{i+1} = b\sin[2(i+1)\pi/n] \tag{6}$$

From the definition of the line segment, the perimeter of the oval profile [18] can be obtained by the following summation:

$$L_{E2} = \sum_{\theta=0}^{2\pi}\sqrt{(x_{i+1}-x_i)^2+(y_{i+1}-y_i)^2} \tag{7}$$

Due to the axial symmetry of the geometry of an oblate spheroid, the external surface area of a bare oblate spheroid container can be obtained by the following summation:

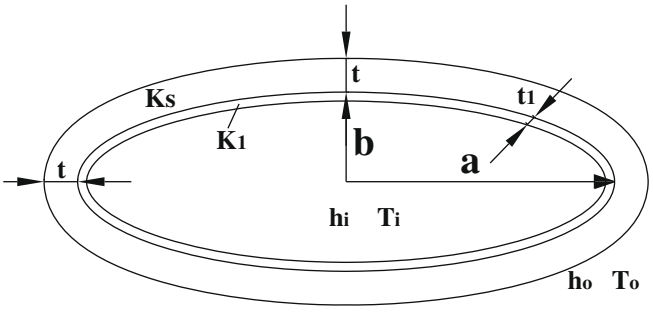

Fig. 1. The parameters of an insulated oblate spheroid container.

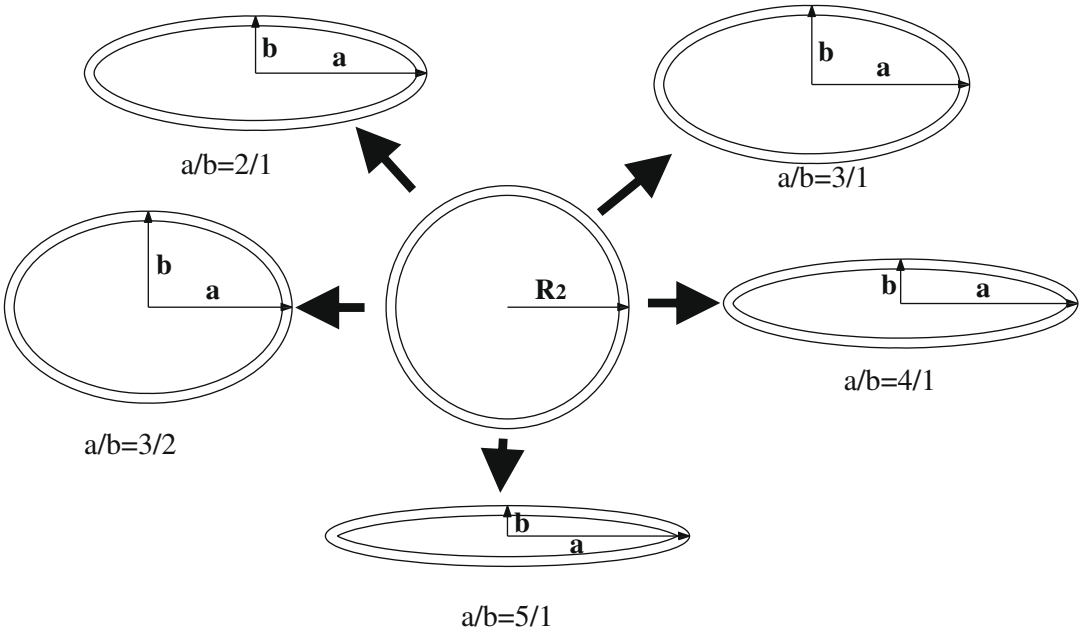

Fig. 2. The oblate spheroid with various long–short-axes ratios *a/b*, transformed from a bare sphere with the same external surface area.

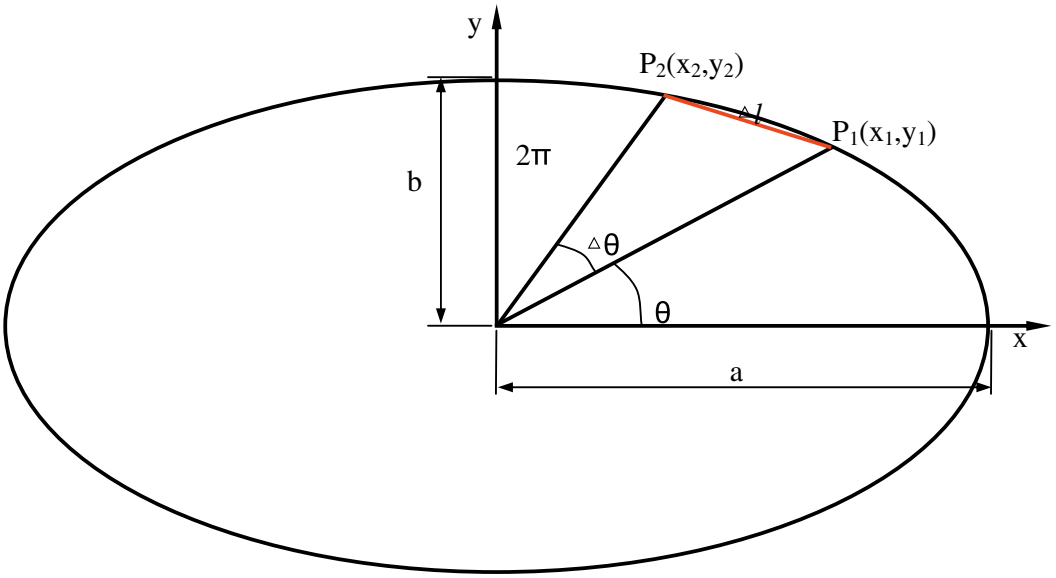

Fig. 3. The oval cross-sectional profile of an oblate spheroid and its relative parameters.

$$A_{E2} = \sum_{\theta=0}^{\pi} 2\pi y_i \sqrt{(x_{i+1} - x_i)^2 + (y_{i+1} - y_i)^2} \tag{8}$$

Similarly, accurate internal oblate spheroid surface area, A_{E1}, can be obtained by replacing the values of a and b by $(a - t_1)$ and $(b - t_1)$, respectively in Eqs. (3)–(6) and (8); meanwhile, accurate external insulation surface area, A_{E3}, can be obtained by replacing the values of a and b by $(a + t)$ and $(b + t)$ in Eqs. (3)–(6) and (8), respectively.

The approximated perimeter and surface area would be highly accurate if the number n is very large. If $a = b = 1$, Eq. (2) becomes a circle. In the case of $n = 10^6$, the error generated from Eq. (7), compared with the exact perimeter of the circle, is about 10^{-5}; and the error generated from Eq. (8), compared with the exact surface area of a sphere ($a = b = 1$), is about 10^{-6}. For the sake of obtaining reliable results, $n = 10^6$ is also adopted in the present investigation to obtain the oblate spheroid surface area. Even with this huge number of segmentations, it only takes only about an insignificant 2 s CPU time in a PC to complete the numerical integration. Due to the extreme small errors generated by Eq. (7) and (8), the approximate values can be regarded as the exact perimeter and surface area.

Since there is no appropriate surface-area formula for an oblate spheroid container, the approximate oval perimeter from Eq. (1) can be extended, to obtain an approximate oblate spheroid surface area as

$$S = 2\pi(a^2 + b^2) \tag{9}$$

By compared with the exact value, the error of oval perimeter generated by Eq. (1) can be expressed as

$$E_L = \frac{L - L_{E2}}{L_{E2}} \times 100\% \tag{10}$$

Similarly, the error of oblate spheroid surface area generated by Eq. (9) can be expressed as

$$E_S = \frac{S - A_{E2}}{A_{E2}} \times 100\% \tag{11}$$

The errors of Eqs. (10) and (11) are shown in Fig. 4. It can be seen that the greater the long-short-axes ratio a/b is, the larger the values of E_L and E_S are. Between them, E_S is much larger than E_L. From Fig. 4, it is obvious that any calculation based on Eq. (9) is inaccurate; therefore, the oblate spheroid surface area shouldn't be obtained by Eq. (9).

2.2. The equivalent sphere based on accurate oblate spheroid surface area

The heat-transfer characteristics of an insulated oblate spheroid can be calculated by using the concept of equivalent sphere based on the same bare external surface area. The outer radius R_2 of the equivalent bare sphere is

$$R_2 = \left(\frac{A_{E2}}{4\pi}\right)^{1/2} \tag{12}$$

R_2 is also used for dimensionless thickness, t/R_2. Since the critical radius of an insulated sphere is $2K_s/h_o$ [15], the dimensionless insulated oblate spheroid container size can be expressed as $0.5R_2h_o/K_s$.

The internal and external surface-areas of equivalent bare sphere are

$$A_{C1} = 4\pi(R_2 - t_1)^2 \tag{13}$$

$$A_{C2} = 4\pi(R_2)^2 = A_{E2} \tag{14}$$

and the external surface area of the equivalent insulated sphere is

$$A_{C3} = 4\pi(R_2 + t)^2 \tag{15}$$

3. The heat transfer rate with one-dimensional *RPSWT* model

The thermal resistance of one-dimensional *RPSWT* model is

$$R_{th} = \frac{t}{K_s\sqrt{A_2A_3}} \tag{16}$$

From Fig. 2, if $a = b$, an insulated oblate spheroid becomes an insulated sphere. Then the relations of t, A_2, and A_3 of an insulated sphere can be written as

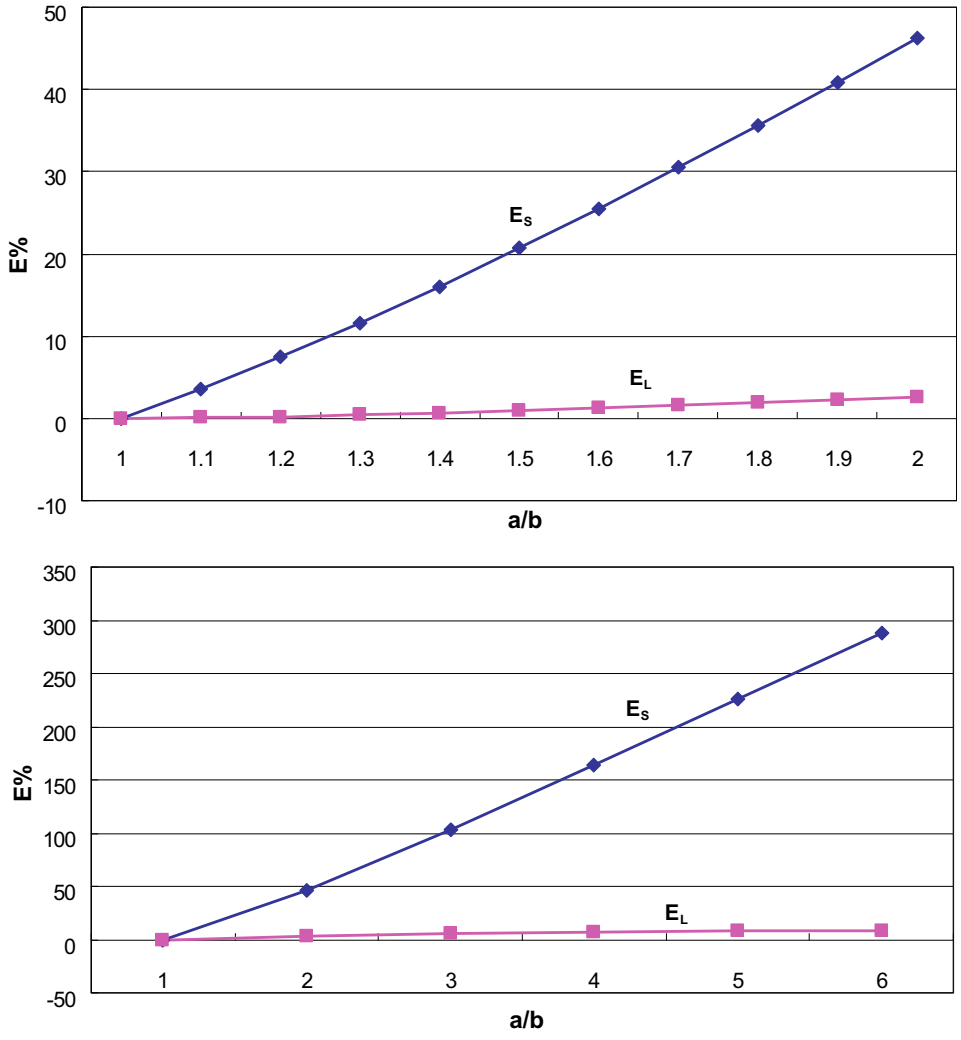

Fig. 4. The errors generated by approximate formulas of oval perimeter and oblate spheroid surface area versus long-short-axes ratio a/b.

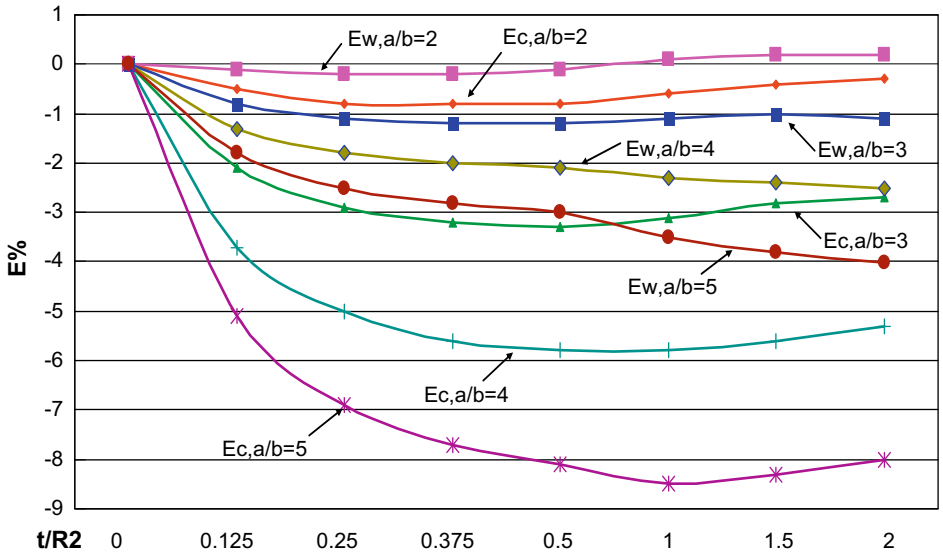

Fig. 5. The relations of E_W and E_C vs. t/R_2 as well as various a/b in situation of dimensionless size $0.5R_2h_o/K_S = 1.55–2.75$ with $h_i = 10^5$ W m^{-2} K^{-1}, $t_1 = 1$ mm, $K_1 = 77$ W m^{-1} K^{-1}, $K_S = 0.035$ W m^{-1} K^{-1}, $h_o = 8.3$ W m^{-2} K^{-1}, $T_i = 100$ °C and $T_o = 0$ °C.

$$t = R_3 - R_2, \quad A_2 = 4\pi R_2^2, \quad \text{and } A_3 = 4\pi R_3^2 \tag{17}$$

Therefore, the thermal resistance of a sphere can also be obtained by substituting Eq. (17) into Eq. (16) as follows

$$R_{th} = \left[\frac{t}{K_s\sqrt{A_2A_3}}\right] = \frac{1}{4\pi K_s}\left(\frac{1}{R_2} - \frac{1}{R_3}\right) \tag{18}$$

It can be seen from Eq. (18) that the thermal resistance of an insulated sphere is a special case of the *RPSWT* model because a sphere can be approached by increasing the number of faces of a polyhedron to infinity.

3.1. Heat transfer rate based on accurate surface area and with RPSWT model

The heat transfer rate of an insulated oblate spheroid container with *RPSWT* model and based on accurate surface area is

$$Q_W = \frac{(T_i - T_o)}{\frac{1}{h_iA_{E1}} + \frac{t_1}{K\sqrt{A_{E1}A_{E2}}} + \frac{t}{K_S\sqrt{A_{E2}A_{E3}}} + \frac{1}{h_oA_{E3}}} \tag{19}$$

And its error compared with three-dimensional numerical heat transfer rate, Q_n, is

$$E_W = \left(\frac{Q_E - Q_n}{Q_n}\right) \times 100\% \tag{20}$$

3.2. Heat transfer rate of an equivalent insulated sphere based on accurate oblate spheroid surface area

The heat transfer rate of an equivalent insulated sphere based on accurate oblate spheroid surface area is

$$Q_C = \frac{(T_i - T_o)}{\frac{1}{h_iA_{C1}} + \frac{1}{4\pi K}\left(\frac{1}{R_1} - \frac{1}{R_2}\right) + \frac{1}{4\pi K_S}\left(\frac{1}{R_2} - \frac{1}{R_3}\right) + \frac{1}{h_oA_{C3}}} \tag{21}$$

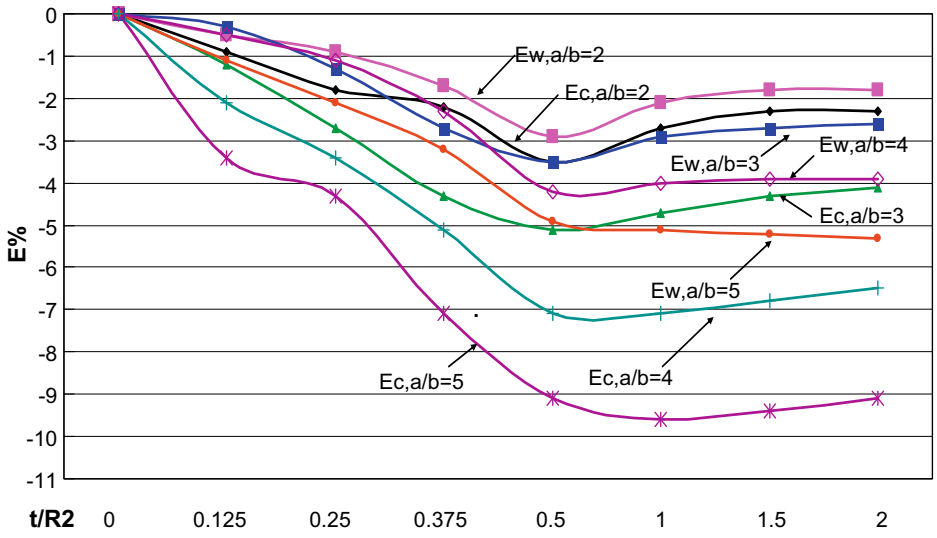

Fig. 6. The relations of E_W and E_C vs. t/R_2 as well as various a/b in situation of dimensionless size $0.5R_2h_o/K_S = 15.5–27.5$ with $h_i = 30$ W m^{-2} K^{-1}, $t_1 = 2$ mm, $K_1 = 77$ W m^{-1} K^{-1}, $K_S = 0.035$ W m^{-1} K^{-1}, $h_o = 8.3$ W m^{-2} K^{-1}, $T_i = 100$ °C and $T_o = 0$ °C.

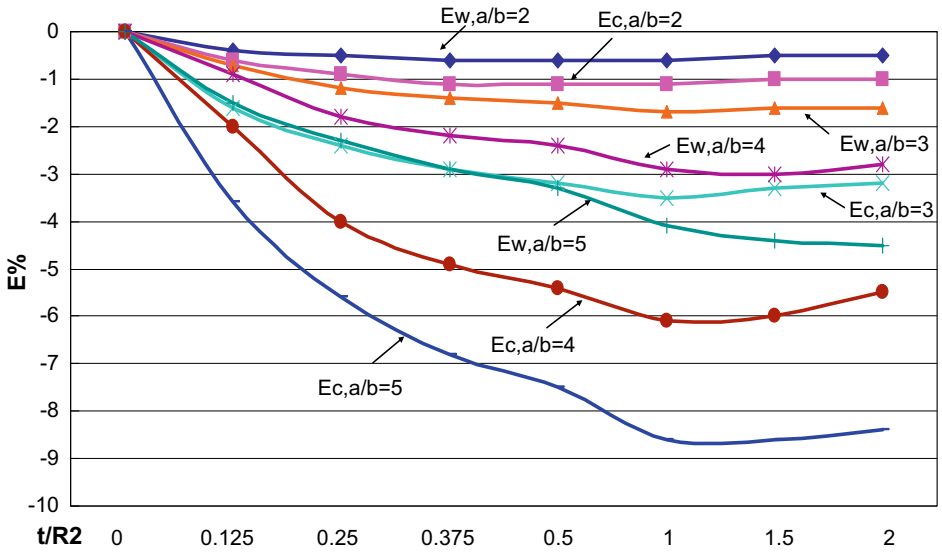

Fig. 7. The relations of E_W and E_C vs. t/R_2 as well as various a/b in situation of dimensionless size $0.5R_2h_o/K_S = 94.8–155.0$ with $h_i = 10^5$ W m^{-2} K^{-1}, $t_1 = 5$ mm, $K_1 = 77$ W m^{-1} K^{-1}, $K_S = 0.035$ W m^{-1} K^{-1}, $h_o = 8.3$ W m^{-2} K^{-1}, $T_i = 100$ °C and $T_o = 0$ °C.

And its error compared with three-dimensional numerical heat transfer rate, Q_n, is

$$E_c = \left(\frac{Q_c - Q_n}{Q_n}\right) \times 100\% \quad (22)$$

4. Energy equation and boundary conditions

The heat conduction governing equation for a three-dimensional insulated oblate spheroid is

Table 1
In situation of $h_i = 10^5$ W m^{-2} K^{-1} with $t_1 = 1$ mm, $K_1 = 77$ W m^{-1} K^{-1}, $K_S = 0.035$ W m^{-1} K^{-1}, $h_o = 8.3$ W m^{-2} K^{-1}, $T_i = 100$ °C and $T_o = 0$ °C, the relations of E_W and E_C vs. t/R_2 as well as various a/b.

t/R_2	t (mm)	Q_W (W m^{-1})	Q_C (W m^{-1})	Q_n (W m^{-1})	E_W (%)	E_C (%)
(a) a/b = 1.5; a = 0.03 m, b = 0.02 m; R_2 = 0.0232 m, $0.5R_2h_o/K_S$ = 2.75						
0	0	5.616	5.616	5.609	0.0	0.0
0.25	5.802	3.231	3.227	3.228	0.1	0.0
0.5	11.60	2.469	2.465	2.464	0.2	0.0
1.0	23.21	1.874	1.871	1.869	0.2	0.1
1.5	34.81	1.625	1.622	1.620	0.3	0.1
2.0	46.41	1.488	1.486	1.4835	0.3	0.2
(b) a/b = 2; a = 0.02 m, b = 0.01 m; R_2 = 0.01307 m, $0.5R_2h_o/K_S$ = 1.55						
0.0	0	1.782	1.782	1.778	0.0	0.0
0.25	3.268	1.423	1.415	1.426	−0.2	−0.8
0.5	6.537	1.215	1.206	1.216	−0.1	−0.8
1.0	13.07	0.997	0.990	0.996	0.1	−0.6
1.5	19.61	0.888	0.882	0.886	0.2	−0.4
2.0	26.15	0.823	0.819	0.821	0.2	−0.3
(c) a/b = 3; a = 0.03 m, b = 0.01 m; R_2 = 0.01567 m; $0.5R_2h_o/K_S$ = 1.858						
0.0	0	2.564	2.564	2.558	0.0	0.0
0.25	3.920	1.888	1.853	1.909	−1.1	−2.9
0.5	7.840	1.556	1.523	1.574	−1.2	−3.3
1.0	15.68	1.241	1.216	1.254	−1.1	−3.1
1.5	23.52	1.092	1.072	1.104	−1	−2.8
2.0	31.36	1.006	0.990	1.017	−1.1	−2.7
(d) a/b = 4; a = 0.04 m, b = 0.01 m; R_2 = 0.0179 m; $0.5R_2h_o/K_S$ = 2.128						
0	0	3.361	3.361	3.353	0	0
0.25	4.488	2.329	2.254	2.373	−1.8	−5
0.5	8.976	1.874	1.804	1.914	−2.1	−5.8
1.0	17.95	1.466	1.413	1.500	−2.3	−5.8
1.5	26.93	1.280	1.238	1.312	−2.4	−5.6
2.0	35.90	1.174	1.140	1.204	−2.5	−5.3
(e) a/b = 5; a = 0.05 m, b = 0.01 m; R_2 = 0.01998 m; $0.5R_2h_o/K_S$ = 2.368						
0	0	4.165	4.166	4.156	0.2	0.2
0.25	4.996	2.749	2.623	2.819	−2.5	−6.9
0.5	9.993	2.173	2.058	2.234	−3	−8.1
1.0	19.99	1.676	1.590	1.737	−3.5	−8.5
1.5	29.98	1.454	1.387	1.512	−3.8	−8.3
2.0	39.97	1.329	1.274	1.385	−4	−8

Table 2
In situation of $h_i = 30$ W m^{-2} K^{-1} with $t_1 = 1$ mm, $K_1 = 77$ W m^{-1} K^{-1}, $K_S = 0.035$ W m^{-1} K^{-1}, $h_o = 8.3$ W m^{-2} K^{-1}, $T_i = 100$ °C and $T_o = 0$ °C, the relations of E_W and E_C vs. t/R_2 as well as various a/b.

t/R_2	t (mm)	Q_W (W m$^{-1)}$	Q_C (W m^{-1})	Q_n (W m$^{-1)}$	E_W (%)	E_C (%)
(a) a/b = 1.5; a = 0.3 m, b = 0.2 m; R_2 = 0.232 m, $0.5R_2h_o/K_S$ = 27.5						
0	0	439.1	439.1	439.1	0.0	0.0
0.25	58.02	47.15	47.10	48.33	−0.3	−0.6
0.5	116.0	29.50	29.46	29.98	−1.6	−1.7
1.0	232.1	20.06	20.03	20.28	−1.1	−1.3
1.5	348.1	16.81	16.79	16.97	−0.9	−1.1
2.0	464.1	15.17	15.15	15.30	−0.8	−1.0
(b) a/b = 2; a = 0.2 m, b = 0.1 m; R_2 = 0.1307 m, $0.5R_2h_o/K_S$ = 15.5						
0	0	139.1	139.2	139.2	0.0	0.0
0.25	32.68	25.14	25.03	26.25	−0.9	−1.8
0.5	65.37	16.21	16.12	16.69	−2.9	−3.5
1.0	130.7	11.18	11.12	11.42	−2.1	−2.7
1.5	196.1	9.411	9.362	9.582	−1.8	−2.3
2.0	261.5	8.506	8.465	8.645	−1.8	−2.3
(c) a/b = 3; a = 0.3 m, b = 0.1 m; R_2 = 0.1568 m; $0.5R_2h_o/K_S$ = 18.6						
0	0	200.2	200.3	200.3	0.0	0.0
0.25	39.20	31.09	30.68	32.51	−1.3	−2.7
0.5	78.40	19.89	19.55	20.60	−3.5	−5.1
1.0	156.8	13.66	13.41	14.07	−2.9	−4.7
1.5	235.2	11.47	11.27	11.78	−2.7	−4.3
2.0	313.6	10.34	10.18	10.61	−2.6	−4.1
(d) a/b = 4; a = 0.4 m, b = 0.1 m; R_2 = 0.1795 m; $0.5R_2h_o/K_S$ = 21.3						
0	0	262.5	262.6	262.5	0	0
0.25	44.88	36.49	35.63	38.26	−1.1	−3.4
0.5	89.76	23.25	22.54	24.26	−4.2	−7.1
1.0	179.5	15.93	15.41	16.59	−4	−7.1
1.5	269.3	13.34	12.94	13.89	−3.9	−6.8
2.0	359.0	12.02	11.68	12.50	−3.9	−6.5
(e) a/b = 5; a = 0.5 m, b = 0.1 m; R_2 = 0.1998 m; $0.5R_2h_o/K_S$ = 23.7						
0	0	325.4	325.6	325.4	0.0	0.0
0.25	49.96	41.47	40.06	43.63	−2.1	−4.3
0.5	99.93	26.38	25.22	27.73	−4.9	−9.1
1.0	199.8	18.04	17.20	19.01	−5.1	−9.6
1.5	299.8	15.09	14.43	15.92	−5.2	−9.4
2.0	399.7	13.57	13.02	14.33	−5.3	−9.1

Table 3
The detail relations of E_W and E_C vs. t/R_2 as well as various a/b in situation of dimensionless size $0.5R_2h_o/K_S = 94.8–155.0$ with $h_i = 105\ W\ m^{-2}\ K^{-1}$, $t_1 = 5$ mm, $K_1 = 77\ W\ m^{-1}\ K^{-1}$, $K_S = 0.035\ W\ m^{-1}\ K^{-1}$, $h_o = 8.3\ W\ m^{-2}\ K^{-1}$, $T_i = 100\ °C$ and $T_o = 0\ °C$.

t/R_2	t (m)	Q_W (W m$^{-1)}$	Q_C (W m^{-1})	Q_n (W m^{-1})	E_W (%)	E_C (%)
(a) a/b = 1.5; a = 1.5 m, b = 1 m; R_2 = 1.16 m, $0.5R_2h_O/K_S$ = 137.6						
0	0	14039	14039	14038	0.0	0.0
0.25	0.290	252.49	252.23	253.08	−0.2	−0.3
0.5	0.580	152.56	152.36	152.97	−0.3	−0.4
1.0	1.160	102.04	101.88	102.27	−0.2	−0.4
1.5	1.740	85.095	84.972	85.276	−0.2	−0.4
2.0	2.320	76.604	76.503	76.762	−0.2	−0.3
(b) a/b = 2; a = 2 m, b = 1 m; R_2 = 1.307 m, $0.5R_2h_O/K_S$ = 155.0						
0.0	0	17825	17825	17822	0.0	0.0
0.25	0.326	285.70	284.57	287.17	−0.5	−0.9
0.5	0.653	172.68	171.76	173.74	−0.6	−1.1
1.0	1.307	115.48	114.82	116.14	−0.6	−1.1
1.5	1.961	96.268	95.752	96.746	−0.5	−1.0
2.0	2.614	86.627	86.205	87.048	−0.5	−1.0
(c) a/b = 3; a = 2.1 m, b = 0.7 m; R_2 = 1.097 m; $0.5R_2h_O/K_S$ = 130.2						
0.0	0	12563	12563	12560	0	0
0.25	0.274	241.53	238.43	244.36	−1.2	−2.4
0.5	0.548	146.58	144.08	148.83	−1.5	−3.2
1.0	1.097	98.158	96.361	99.804	−1.7	−3.5
1.5	1.646	81.77	80.373	83.127	−1.6	−3.3
2.0	2.194	73.505	72.363	74.717	−1.6	−3.2
(d) a/b = 4; a = 2 m, b = 0.5 m; R_2 = 0.898 m; $0.5R_2h_O/K_S$ = 106.4						
0	0	8402.2	8402.3	8400.5	0.0	0.0
0.25	0.224	199.06	194.47	202.66	−1.8	−4.0
0.5	0.448	121.41	117.70	124.43	−2.4	−5.4
1.0	0.897	81.439	78.771	83.850	−2.9	−6.1
1.5	1.346.	67.790	65.715	69.887	−3.0	−6.0
2.0	1.796	60.867	59.171	62.643	−2.8	−5.5
(e) a/b = 5; a = 2 m, b = 0.4 m; R_2 = 0.799 m; $0.5R_2h_O/K_S$ = 94.8						
0	0	6664.7	6664.8	6663.3	0.0	0.0
0.25	0.199	178.87	172.88	183.12	−2.3	−5.6
0.5	0.399	109.57	104.74	113.28	−3.3	−7.5
1.0	0.799	73.611	70.135	76.730	−4.1	−8.6
1.5	1.199	61.226	58.518	64.025	−4.4	−8.6
2.0	1.598	54.908	52.694	57.524	−4.5	−8.4

$$\frac{\partial}{\partial x}\left(K\frac{\partial T}{\partial x}\right)+\frac{\partial}{\partial y}\left(K\frac{\partial T}{\partial y}\right)+\frac{\partial}{\partial z}\left(K\frac{\partial T}{\partial z}\right)=0 \tag{23}$$

The boundary conditions are

$$h_i(T_i - T_{sA_1}) = -K\left(\frac{\partial T}{\partial N}\right)_{A_1} \tag{24}$$

$$-K_s\left(\frac{\partial T}{\partial N}\right)_{A_3} = h_o(T_s - T_o)_{A_3} \tag{25}$$

$$\left(\frac{\partial T}{\partial N}\right)_{\text{symmetrical.boundary}} = 0 \tag{26}$$

where N is the normal direction on any surface, and T_s represents the surface temperature of the insulation layer.

5. Numerical two-dimensional heat-transfer results

Eqs. (23)–(26) are solved by an in-house USTREAM code developed by the third named author to obtain the three-dimensional numerical heat-transfer results. In order to check if the numerical results are reliable, an insulated sphere is analyzed to determine how many cells are needed to obtain a satisfactory result. It was found that a model of an insulated sphere, which consists of 26,600 cells, gave a satisfactory solution of heat transfer rate within ±0.01% compared with that from exact analytic solution. Therefore, in the case of analyzing an insulated oblate spheroid, the numerical solutions obtained by the model with same number of cells can be expected to be highly accurate.

6. Results and discussion

The results of the oblate spheroid container with various long–short-axes ratios a/b of 1.5, 2, 3, 4 and 5 in practical situations of external convection heat transfer coefficients $h_o = 8.3\ W\ m^{-2}\ K^{-1}$, wall conductivity $K_1 = 77\ W\ m^{-1}\ K^{-1}$, insulation layer conductivity $K_S = 0.035\ W\ m^{-1}\ K^{-1}$, internal fluid temperature $T_i = 100\ °C$ and external fluid temperature $T_o = 0\ °C$ with various dimensionless container size ($0.5R_2h_o/K_s$) and internal heat convection coefficient h_i are shown in Figs. 5–7 and Tables 1–3, respectively. The relations of heat transfer rate error, E_W, calculated by one-dimensional *RPSWT* model with accurate surface area, and heat transfer rate error, E_C, of an insulted equivalent sphere based on accurate external surface area of a bare oblate spheroid versus dimensionless insulated thickness, t/R_2, in situation of dimensionless container size, $0.5R_2h_o/K_S = 1.55–2.75$, with $h_i = 10^5\ W\ m^{-2}\ K^{-1}$ are shown in Fig. 5 and Table 1, which lists the detail data. The relations of E_W and E_C vs. t/R_2 in cases of $0.5R_2h_o/K_S = 15.5–27.5$ with $h_i = 30\ W\ m^{-2}K^{-1}$ are shown in Fig. 6 and Table 2. The relations of E_W and E_C vs. t/R_2 in cases of $0.5R_2h_o/K_S = 94.8–155.0$ with $h_i = 10^5\ W\ m^{-2}\ K^{-1}$ are shown in Fig. 7 and Table 3.

It is found from Figs. 5–7 and Tables 1–3 that in situations of $a/b \leqq 3$ and $t/R_2 \leqq 2$, $E_W \leqq 3\%$; and in other rarer situations with $a/b \leqq 5$ and $t/R_2 \leqq 2$, $E_W \leqq 5.5\%$, the results are almost independent with the convective coefficient of internal fluid h_i and dimensionless container size if a model is based on accurate external surface area of a bare oblate spheroid. However, the heat transfer rate errors, E_C are almost twice as large as those of E_W.

7. Conclusions

This study shows that approximate surface-area formula is not suitable to be applied to an insulated oblate spheroid to obtain reliable heat-transfer results. In order to achieve a higher level of accuracy, an integration method, which returns very accurate surface area, introduced in this study needs to be used. Since using equivalent sphere based on the same external surface area of a bare oblate spheroid generates higher errors, reliable one-dimensional *RPSWT* model based on accurate surface area should be employed to calculate the heat transfer characteristic of an insulated oblate spheroid container. This only requires a PC incorporated with a small computer code in any language (such as LabVIEW in this study) without the need to use CFD software. As demonstrated in this study, reliable heat-transfer results can easily be obtained by this simple practice. It is very suitable to engineering application.

Acknowledgment

The authors would like to thank the National Science Council of Taiwan, ROC for the financial support of this study, which was completed under the Project numbered NSC-97-2221-E168-044-MY2.

References

[1] Holman JP. Heat transfer. 8th SI metric ed. McGraw-Hill Inc.; 2001. p. 7–39 and 638–42.
[2] Pita EG. Air conditioning principles and system. 3rd ed. Prentice Hall; 1998. p. 252–6..
[3] Stoecker WF, Jones JW. Refrigration and air conditioning. 2nd ed. McGraw-Hill; 1982. p. 24–35.
[4] Dossat RJ. Principles of refrigeration. 3rd ed. Prentice Hall; 1991. p. 167–78.
[5] Chatenever R. Air conditioning and refrigeration for the professional. John Wiley & Sons Inc.; 1988. p. 445–8.
[6] Chou HM, Wong KL. Heat transfer characteristics of an insulated regular polygonal duct by using a wedge thermal resistance model. Energy Convers Manage 2003;44:629–45.
[7] Wong KL, Chou HM, Li YH. Complete heat transfer solutions of an insulated regular polygonal duct by using a PWTR model. Energy Convers Manage 2004;45:1705–24.

[8] Wong KL, Hsien TL, Richards P, Her BS. The reliable simple one-dimensional 64-CPWTR model applied to the two-dimensional heat transfer problem of an insulated rectangular duct in an air conditioning or refrigeration system. Int J Refrig 2005;28:1029–39.
[9] Wong KL, Chen WL, Tsai JC, Lu TH. The reliable simple one-dimensional 46-CPWTR model applied to the two-dimensional heat transfer problem of an insulated triangular duct. Energy Convers Manage 2007;48(12):3135–45.
[10] Wong KL, Al-Jumaily A, Lu TH. Reliable one-dimensional CPWTR models for two-dimensional insulated polygonal ducts. Int J Refrig 2007;30:254–66.
[11] Wong KL, Chou HM, Li YH. The optimum interior area thermal resistance model to analyze the heat transfer characteristics of an insulated container with arbitrary shape. Energy Convers Manage 2004;45:963–82.
[12] Wong KL, Chou HM. The heat transfer characteristics of an insulated regular cubic box by using a solid wedge thermal-resistance model. Energy Convers Manage 2003;44:1983–97.
[13] Wong KL, Chou HM, Her BS, Yeh HC. Complete heat transfer solutions of an insulated regular cubic tank with a SWTR model. Energy Convers Manage 2004;45:2813–31.
[14] Wong KL, HM Chou. Heat transfer characteristics of an insulated regular polyhedron by using a regular polygonal top solid wedge thermal resistance model. Energy Convers Manage 2003;44:3015–36.
[15] Lee JF, Wong KL, Chen WL, Ku SS. Complete heat transfer solutions of an insulated regular polyhedron by using a RPSWT model. Energy Convers Manage 2005;46:2232–57.
[16] Chen WL, Wong KL, Chou HM. A reliable one-dimensional method applied to heat-transfer problems associated with insulated rectangular tanks in refrigeration systems. Int J Refrig 2006;29:285–94.
[17] Chen WL, Wong KL. A reliable analytical method applied to heat transfer problems associated with insulated cylindrical tanks. Energy Convers Manage 2007;48:679–87.
[18] Chen WL, Wong KL, Hsien TL, Huang CT. Reliable one-dimensional approximate solution of an insulated oval duct. Energy Convers Manage 2007;48:3135–45.
[19] William HB. CRC standard mathematical table. 25th ed. Cleveland: Chemical Rubber Pub.; 1978. p. 14.